Functional Impact of Genomic Complexity on the Transcriptome of Multiple Myeloma

Bachisio Ziccheddu[1,2], Matteo C. Da Via[3,4], Marta Lionetti[3,4], Akihiro Maeda[4], Silvia Morlupi[4], Matteo Dugo[5], Katia Todoerti[3,4], Stefania Oliva[1], Mattia D'Agostino[1], Paolo Corradini[4,6], Ola Landgren[2,7,8], Francesco Iorio[9,10], Loredana Pettine[3], Alessandra Pompa[3], Martina Manzoni[3,4], Luca Baldini[3,4], Antonino Neri[3,4], Francesco Maura[2,7,8], and Niccolò Bolli[3,4]

ABSTRACT

Purpose: Multiple myeloma is a biologically heterogenous plasma-cell disorder. In this study, we aimed at dissecting the functional impact on transcriptome of gene mutations, copy-number abnormalities (CNA), and chromosomal rearrangements (CR). Moreover, we applied a geno-transcriptomic approach to identify specific biomarkers for personalized treatments.

Experimental Design: We analyzed 514 newly diagnosed patients from the IA12 release of the CoMMpass study, accounting for mutations in multiple myeloma driver genes, structural variants, copy-number segments, and raw-transcript counts. We performed an *in silico* drug sensitivity screen (DSS), interrogating the Cancer Dependency Map (DepMap) dataset after anchoring cell lines to primary tumor samples using the *Celligner* algorithm.

Results: Immunoglobulin translocations, hyperdiploidy and chr(1q)gain/amps were associated with the highest number of deregulated genes. Other CNAs and specific gene mutations had a lower but very distinct impact affecting specific pathways. Many recurrent genes showed a hotspot (HS)-specific effect. The clinical relevance of double-hit multiple myeloma found strong biological bases in our analysis. Biallelic deletions of tumor suppressors and chr(1q)-amplifications showed the greatest impact on gene expression, deregulating pathways related to cell cycle, proliferation, and expression of immunotherapy targets. Moreover, our *in silico* DSS showed that not only t(11;14) but also chr(1q)gain/amps and *CYLD* inactivation predicted differential expression of transcripts of the BCL2 axis and response to venetoclax.

Conclusions: The multiple myeloma genomic architecture and transcriptome have a strict connection, led by CNAs and CRs. Gene mutations impacted especially with HS-mutations of oncogenes and biallelic tumor suppressor gene inactivation. Finally, a comprehensive geno-transcriptomic analysis allows the identification of specific deregulated pathways and candidate biomarkers for personalized treatments in multiple myeloma.

Introduction

Multiple myeloma is a plasma-cell neoplasm driven by recurrent trisomies- hyperdiploid multiple myeloma (HDMM)- or by immunoglobulin gene (IGH) locus rearrangements promoting overexpression of recurrent oncogenes. Classic PCR and FISH studies, and more recently next-generation sequencing (NGS) studies have highlighted a vast array of additional mutations, copy-number abnormalities (CNA) and structural variants (SV) which are thought to play a role in disease evolution and may be acquired in preclinical phases or at relapse after treatment (1–9).

Such abnormalities are predicted to influence the biological and clinical behavior of the tumor and yet, despite a clear driver role, only few carry prognostic value (2, 10–12). Additionally, as the genomic makeup of multiple myeloma is being comprehensively elucidated by NGS studies, classification efforts seem to have gained very little by the additional knowledge brought by NGS and initiating karyotypic events are still the mainstay of multiple myeloma classification. Indeed, most additional abnormalities discovered by NGS seem to be randomly distributed with few notable exceptions (13, 14) and their discovery has not led to the characterization of additional multiple myeloma categories so far. If not relevant from the point of view of a genomic classification then, a question is what their biological role really is, and whether they can serve as markers of specific transcriptional profiles.

Classically, gene-expression profiling arrays have shown how transcriptome profiling recapitulates the main karyotypic lesions in multiple myeloma (15–17). Few studies on RNA sequencing (RNA-seq) in multiple myeloma have been published (7, 14, 18–21). Most of them have reported that many DNA mutations are actually not expressed, and how the transcriptomic profile has very few genomic correlates

[1]Department of Molecular Biotechnologies and Health Sciences, University of Turin, Turin, Italy. [2]Multiple Myeloma Program, Sylvester Comprehensive Cancer Center, University of Miami Health System, Miami, Florida. [3]Hematology Unit, Fondazione IRCCS Ca' Granda Ospedale Maggiore Policlinico, Milan, Italy. [4]Department of Oncology and Hemato-Oncology, University of Milan, Milan, Italy. [5]Platform of Integrated Biology, Department of Applied Research and Technology Development, Fondazione IRCCS Istituto Nazionale dei Tumori, Milan, Italy. [6]Department of Clinical Oncology and Hematology, Fondazione IRCCS Istituto Nazionale dei Tumori, Milan, Italy. [7]Myeloma Service, Department of Medicine, Memorial Sloan Kettering Cancer Center, New York, New York. [8]Department of Medicine, Weill Cornell Medical College, New York, New York. [9]Centre for Computational Biology, Human Technopole, Milan, Italy. [10]Cancer, Ageing and Somatic Mutation Programme, Wellcome Sanger Institute, Cambridge, United Kingdom.

Note: Supplementary data for this article are available at Clinical Cancer Research Online (http://clincancerres.aacrjournals.org/).

B. Ziccheddu and M.C. Da Via contributed equally to this article.

F. Maura and N. Bolli jointly supervised the work.

Corresponding Authors: Francesco Maura, Multiple Myeloma Program, Sylvester Comprehensive Cancer Center, University of Miami Health System, 1120 North-West 14th Street, Miami, FL 33136. Phone: 305-243-7687; E-mail: fxm557@med.miami.edu; and Niccolò Bolli, Department of Oncology and Hemato-Oncology, University of Milan, Via Francesco Sforza 35, Milan 20122, Italy. Phone: 3902-5503-3337; E-mail: niccolo.bolli@unimi.it

Clin Cancer Res 2021;27:6479–90

doi: 10.1158/1078-0432.CCR-20-4366

Translational Relevance

In this article, we studied the close interactions between the genomic architecture of multiple myeloma and its functional impact on the transcriptome. This comprehensive analysis highlighted how copy-number changes and chromosomal rearrangements impacted the most on gene expression. However, we showed the great importance that mutations play in the setting of hotspot variants and biallelic inactivation of tumor suppressor genes. Moreover, a widespread geno-transcriptomic analysis was able to infer the differential gene expression of specific druggable pathways and to identify biomarkers of sensitivity to novel treatments in multiple myeloma, suggesting this approach could drive personalized treatment decisions.

aside from hyperdiploidy and IGH translocations. Laganà and colleagues have shown that RNA-seq from the public CoMMpass database can be mined through a network approach to identify multiple myeloma groups where annotation of genomic and clinical features highlights some commonalities (20). However, a systematic and comprehensive assessment of the functional impact of mutations, CNAs and SVs at the transcriptomic level is still lacking. This would have implications for disease pathogenesis and would allow prioritization of research on genomic abnormalities that have specific consequences on expression. Ideally, those would be the ones with the highest value as prognostic markers, biomarkers of drug response, and/or candidate drug targets. Indeed, while for example response to venetoclax is best predicted by assessing the expression levels of *BCL2*, *BCL2L1*, and *MCL1* (22), this is unlikely to become routine clinical practice. DNA abnormalities that correlate with expression of target genes are much more easily amenable to clinical-grade diagnostics through NGS techniques (23–25).

In this article, we mined genomic and transcriptomic data from 514 cases from the CoMMpass dataset to dissect transcriptional effects of the most recurrent genetic abnormalities. In particular, starting from the comprehensive DNA exome-wide sequencing information, we performed a systematic and unbiased assessment of differentially expressed transcripts correlated to each recurrent gene mutation, CNA and SV. From here, we identified genetic predictors of specific differential gene expression levels to get insights into the functional relevance of recurrent genomic alterations and suggest therapeutic vulnerabilities.

Materials and Methods

Data

We interrogated 514 newly diagnosed patients enrolled in the CoMMpass study (IA12 release). The CoMMpass data were generated as part of the Multiple Myeloma Research Foundation (MMRF) Personalize Medicine Initiative (https://themmrf.org). We focused on mutations in multiple myeloma driver genes, SVs, copy number segments, and raw transcript counts. The CoMMpass trial is a prospective observational clinical trial (NCT01454297) that comprises whole genomic and transcriptomic data derived from newly diagnosed patients with multiple myeloma. The tumor samples were collected from several centers across the United States, Canada and Europe. Ethics committees or institutional review boards at the study sites approved the study. All the patients signed a written informed consent prior to enrollment. The study was conducted under the statement of the Helsinki declaration. Multiple myeloma samples were collected at diagnosis at enrollment sites and then shipped to the Translational Genomics Research Institute (TGen) to be processed and sequenced. Due to the lack of transcriptomic data from normal plasma cells in the CoMMpass dataset, all the statistical analyses were performed comparing genetic subsets of multiple myeloma samples.

Gene expression analysis

RNA-seq data were processed using the *voom*/*limma* pipeline (26, 27). Firstly, the dataset of raw-counts was filtered to remove genes with less than 10 reads in more than 95% of samples. Then, we performed the trimmed mean of M-values (TMM) normalization to estimate a scale factor used to decrease technical bias between samples, resulting from differences in library size (28). Finally, we applied the *voom* transformation to convert the raw counts in log2-counts per million ($\log_2$-CPM) and calculated the respective observation-level weights to be used in differential expression analysis.

To assess the amount of differentially expressed transcripts a linear model was fitted to the expression data for each genomic feature, detecting the genes significantly associated with at least one genetic abnormality. This model evaluates the expression of each gene in each patient using a design matrix composed of information on genetic anomalies for each patient. From this, we obtained the coefficients that measure the gene expression change associated with the presence of each genetic anomaly. Then, to determine the association between gene expression and genomic alterations we used the F statistic obtained by the *lmFit* function of the R *limma* package. Finally, we applied the Benjamini–Hochberg correction for multiple testing. To evaluate the accuracy of the applied model, we calculated a random model in which all the values of each covariate (genetic anomaly) were randomly permuted, breaking all the correlations between the gene expression level and genotype (29). This model allowed to correct the subsequent differential expression analysis for the main karyotypic subtypes and segmental CNAs [hyperdiploidy, t(4;14), t(11;14), t(14;16), t(14;20) and chr(1q21)gains/amplifications (amp)]. Moreover, this approach allowed us to identify significant gene associations by calculating the coefficient of determination (R^2), which tells how well the model fits the data, but also the portion of variance of the dependent variable (expression of gene in a patient) predicted by the independent variable (presence of genetic anomaly). This allowed us to measure the variance explained by the presence/absence of a given genetic alteration and to evaluate how much this alteration is associated with changes in expression of the candidate gene.

Hotspot and non-hotspot mutations

Mutational hotspots (HS) are amino acid positions in a protein-coding gene mutated more frequently than would be expected in the absence of selection (30), therefore conferring a fitness advantage. For this analysis, we selected 4 genes from a list of 53 mutations on known myeloma driver genes (13): *KRAS*, *NRAS*, *IRF4*, and *BRAF*. Then, we defined as HS the nonsynonymous mutations as follows: G12, G13, and Q61 were selected as HS for *KRAS* and *NRAS*; K123 for *IRF4*; and V600 and D594 codons for *BRAF*.

Identification of genes with a cumulative effect

Cumulative transcriptomic effect of genes was analyzed in regions of chr(1q21) amplifications (>3 copies) or biallelic inactivation of tumor suppressors (mutation of one copy and deletion of the other). To explore the functional significance of these events, we selected genes with a cumulative effect, i.e., genes significantly deregulated in biallelic versus wild-type (WT) [or amp vs. WT for chr(1q21)] and/or biallelic

versus mono-allelic statuses [or amp vs. gain for chr(1q21)]. To perform this analysis, first we selected, for each analysis, the significant genes from the differential expression analysis contrasts, then for each selected gene we calculated with a linear regression their cumulative effect. Finally, we restricted the analysis to the significant genes (P value < 0.05) deregulated in biallelic (or amp) versus WT and/or biallelic (or amp) versus mono-allelic (or gain).

Gene ontology analysis

The Gene Ontology (GO) enrichment analysis was performed using *ClusterProfiler* R package to search for a biological interpretation of transcriptome deregulation. This algorithm implements methods to analyze and visualize functional profiles of genomic coordinates, genes, and gene clusters (31). The P values were corrected for multiple testing by using the Benjamini–Hochberg FDR method. In the HS analysis, we performed the pathway analysis with the genes from differential expression analysis contrasts (HS vs. WT, HS vs. non-HS, and non-HS vs. WT); whereas in the biallelic deletions and chr(1q21) gain/amp analysis, we executed the GO analysis with the cumulative effect genes. Gene set enrichment analysis (GSEA) was performed by the R package *fgsea* using the "t" statistics as ranking factor. The cancer hallmark list was inferred with a significant adjusted P value < 0.05 (32).

In silico analysis of drug sensitivity

To assess our findings, we performed an *in silico* analysis using the Cancer Dependency Map (DepMap) database and *Celligner* algorithm (detailed methods in the Supplementary Data S1; refs. 33–35).

Statistical analysis

The association tests have been performed with two-sided Wilcoxon rank–sum test. The P values were adjusted using the Benjamini–Hochberg FDR method (FDR<0.05). All analyses were performed in R, the language and environment for statistical computing (R Core Team, 2020).

Results

Genome-wide transcriptome patterns associated with multiple myeloma driver aberrations

To have an overview of the driver genomic lesions underlying global transcriptome deregulation in multiple myeloma, we first performed an unsupervised principal component analysis. Cases segregated mostly based on their HD versus IGH translocation status (**Fig. 1A**), in agreement with historical gene expression profiling data (15, 17, 36, 37). However, recent genomic efforts have greatly expanded the repertoire of driver genomic lesions in multiple myeloma, including CNAs and gene mutations. Therefore, we asked what the independent contribution of each to the derangement of the transcriptome could be. To this end, we implemented a linear regression model that assesses which transcripts are specifically associated to distinct genomic features (29). We plotted, for each driver lesion, the number of up- or downregulated transcripts and their fold change (**Fig. 1B**). IGH translocations and hyperdiploidy were associated overall with the most substantial differential gene expression patterns observed, along with amplifications and gains in chr(1q21). Other CNAs had fewer transcriptomic correlates, followed by specific gene mutations. Within the former group, *CYLD* deletions showed the highest number of differentially expressed transcripts compared with normal *CYLD* copy number (CN) status. Mutations of the 53 known driver genes in multiple myeloma (13) were characterized by less consistent transcriptomic patterns. However, interesting correlations emerged from this analysis. *DIS3* and *NRAS* mutations were the two lesions whose occurrence was associated with the largest transcriptional modulation with respect to germline configuration. A high number of differentially expressed long noncoding RNA (lncRNA) was observed in *DIS3*-mutated versus WT patient samples in particular, confirming DIS3 may mostly regulate expression at the post-transcriptional level (Supplementary Data S2; ref. 38). As expected, GO analysis for *NRAS* and *KRAS* mutations showed differential expression of genes pertaining to the MAPK pathway (Supplementary Fig. S1A and S1B). Among less frequent mutations, *TGDS* and *RB1* in 13q and the *MYC* transcriptional regulators *IRF4* and *MAX* displayed correlation with the transcriptome. Conversely, most of the remaining gene mutations were not associated with any differentially expressed transcript.

IGH translocations exert their transforming activity by overexpressing target oncogenes. Indeed, modelling predicted versus observed expression of *CCND1* showed that the t(11;14) accounted for most of the observed inter-patient heterogeneity in *CCND1* transcript levels (**Fig. 1C**, left), as was the case for *NSD2* and to a lesser extent *FGFR3* expression in t(4;14), *MAF* in t(14;16), and *MAFB* in t(14;20) (Supplementary Fig. S2A–S2D). In the case of CNAs, the picture was not as clear cut: while low *CYLD* expression levels were mostly explained by locus deletions (**Fig. 1C**, right), not all cases of chr(17p13) or *TRAF3* gene deletions resulted in downregulation of *TP53* or *TRAF3*, respectively (Supplementary Fig. S2E and S2F). In the case of chr(1q21)gain/amp, heterogeneity of expression levels of the key target genes *CKS1B* and *MCL1* could be attributed to the allelic status of the locus only to an extent (Supplementary Fig. S2G and S2H).

Therefore, structural, numeric variants and few mutations in driver genes were associated with most of the transcriptomic heterogeneity between multiple myeloma cases. For canonical IGH translocations this is likely mediated by overexpression of the target oncogene. The transcriptomic inter-patient variability observed in the case of CNAs is likely associated with the altered expression of more than one target gene and can be partially explained by the clonality of the event.

Impact of driver recurrent gene mutations on gene-expression regulation

Despite having a smaller correlation with the transcriptome, recurrent gene mutations have a clear driver role. Many genes are mutated in a HS pattern, and specific effects of HS versus non-HS variants as compared to their WT status are unknown. We therefore sought to analyze genotype–phenotype correlations for 4 of the main mutated genes with known HS: *KRAS*, *NRAS*, *BRAF*, and *IRF4*. The distribution of HS and non-HS mutations within the main cytogenetic categories was neutral except for kinase-dead *BRAF* mutations at codon D594, mostly occurring in t(14;16) cases (Supplementary Fig. S3). As a first step, we interrogated the Catalogue of Somatic Mutations in Cancer (COSMIC) to interrogate the codon usage of these gene mutations in CoMMpass as compared with different solid cancer types (colon, lung adenocarcinoma, and skin melanoma) and other hematologic malignancies. Interestingly, multiple myeloma showed a specific mutational spectrum for some of these genes. *KRAS* in particular was mostly mutated in the Q61 codon in multiple myeloma, while in solid cancers, diffuse large B-cell lymphomas, chronic lymphocytic leukemia (CLL), and acute myeloid leukemia (AML) showed mostly G12 and G13 mutations (**Fig. 2A**; Supplementary Fig. S4A). *NRAS* was mainly mutated at the Q61 codon. A similar picture was also observed for solid cancers. However, in this latter setting, G12 and G13 residues mutations were also enriched in comparison with multiple myeloma

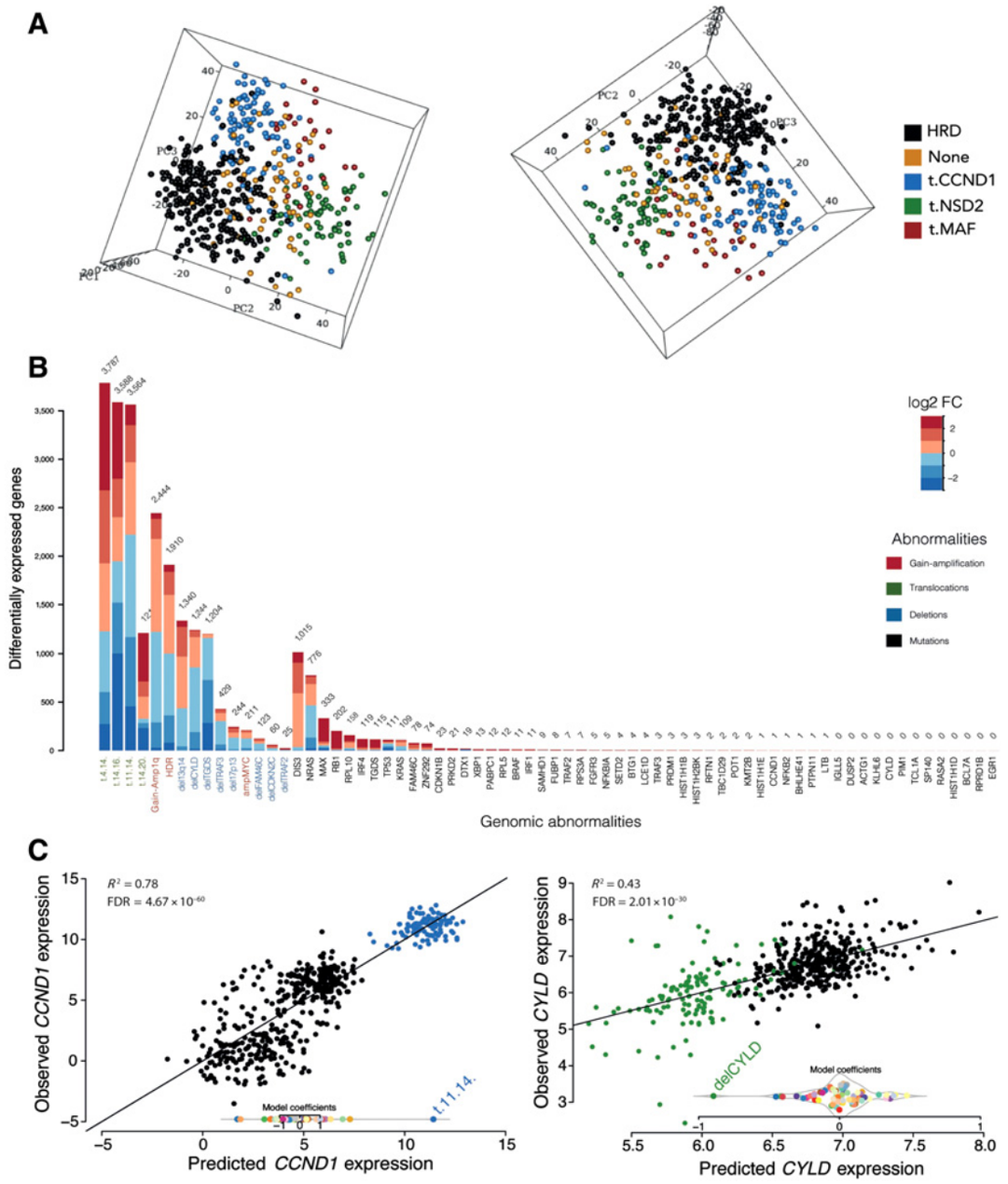

Figure 1.

Transcriptomic profile. **A,** Principal component analysis based on the main karyotypic subtypes: samples are represented as dots in the space identified by the three principal components and are color-coded based on their karyotype. **B,** Stacked bar chart showing the differentially expressed genes per each genomic abnormality (FDR < 0.05, fold change cut-off 1.5). Bars indicate the contributions of upregulated genes (red) and downregulated genes (blue). FC, fold change. **C,** Scatterplot representing expression prediction for the *CCND1* and *CYLD* genes versus observed expression values: samples are color-coded dots based on the significant genomic abnormality (FDR < 0.01), in blue t(11;14) samples, in green del(*CYLD*) samples and in black the other samples; R^2 represents the association between genomic alteration and expression changes.

(**Fig. 2B**). Interestingly, other hematologic malignancies showed a predominance of *NRAS* G12 and G13 mutations, and only CLL showed a mutational pattern similar to multiple myeloma (Supplementary Fig. S4B). The *IRF4* K123 HS was specific for multiple myeloma. Nevertheless, we identified other *IRF4* mutated HS in B and in T-cell neoplasms, all within the DNA binding domain. In solid cancers, where *IRF4* is not usually expressed, we did not identify any clustered mutational locus (**Fig. 2C**; Supplementary Fig. S4C). Finally, while *BRAF* mutations were mostly clustered on the V600, multiple myeloma and other hematologic malignancies showed a higher incidence of the "kinase-dead" D594 mutations as compared with solid tumors (**Fig. 2D**; Supplementary Fig. S4D). Notable exceptions were

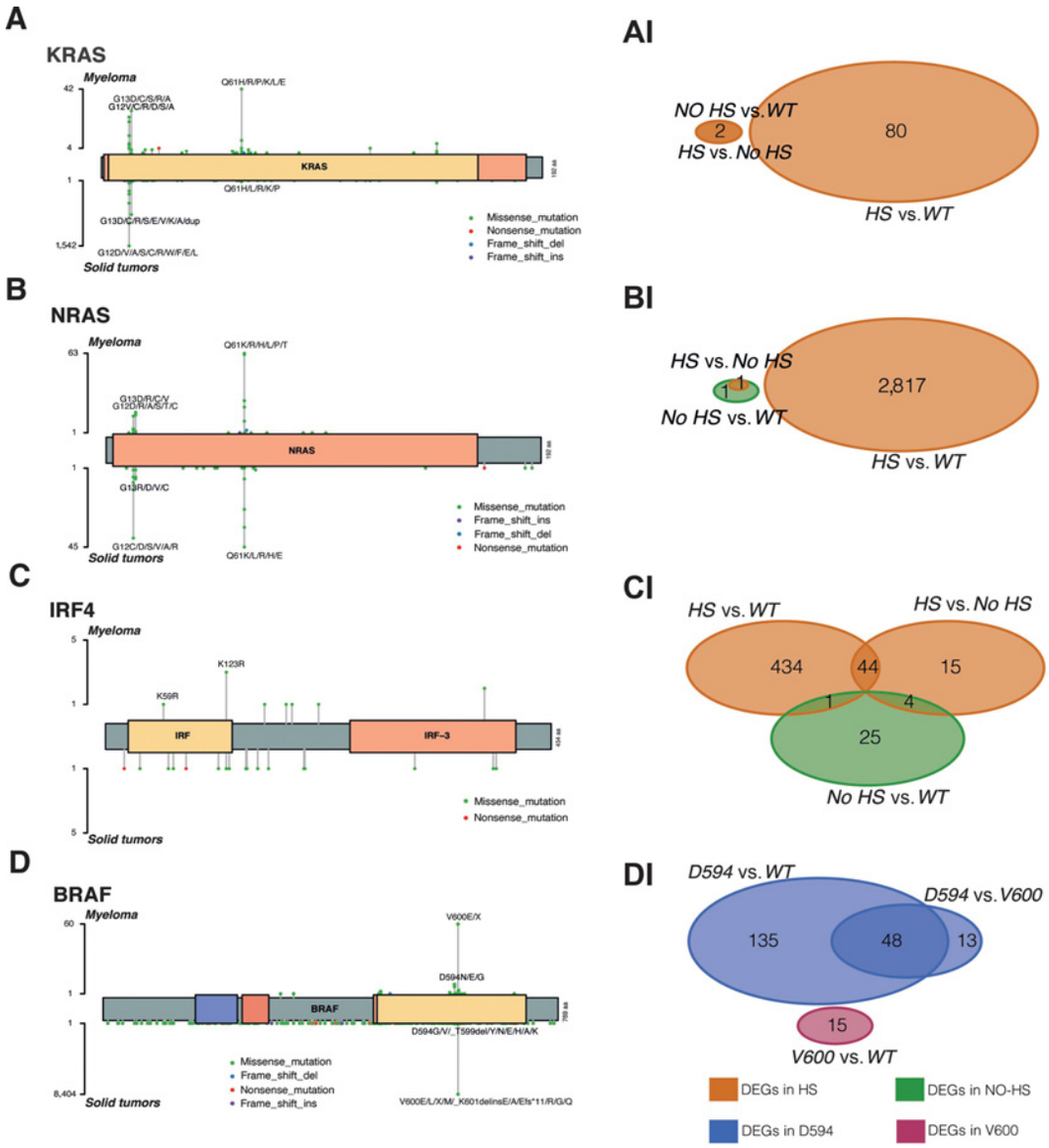

Figure 2.

Hotspot versus non-HS and WT analysis. **A–D,** Lollipop plots for the four main mutated genes; each plot shows in the top the hotspots in multiple myeloma, at the bottom the hotspots in the peculiar solid cancers. Lollipop plots have been generated applying the R package *maftools*. **AI–DI,** Venn plots for each differential expression analysis.

hairy cell leukemia and Langherans' histiocytosis, where only the V600 residue mutated (Supplementary Fig. S4D).

Next, we asked whether HS and non-HS mutations would carry different functional relevance as assessed by transcriptomic analysis: for *KRAS* and *NRAS*, we found transcriptomic correlates for HS gene mutations only. Interestingly, even if the two genes fuel the same proliferative pathway (Supplementary Fig. S1), *NRAS* HS mutations were associated with differential expression of more than 2,000 genes, as compared with 80 for *KRAS* HS mutations (**Fig. 2AI, BI**; Supplementary Fig. S5A and S5B). In the case of *IRF4*, again HS mutations correlated with the highest number of differentially expressed transcripts, while non-HS mutations were characterized by a less substantial and partly overlapping transcriptional profile (**Fig. 2CI**; Supplementary Fig. S5C). Interestingly, for *BRAF* mutations, the D594 codon was correlated with the highest level of differential gene expression, showing some overlap with mutations in the canonical codon V600. In particular, the kinase-dead mutations at D594 were associated with the differential expression of 183 genes, three times more than the V600 ones. This may be partly explained by the specific occurrence of D594 mutations in *MAF*-translocated multiple myeloma subgroup (4/7 cases) as previously described (14). Overall, non-HS mutations contributed very little in *BRAF* (**Fig. 2DI**; Supplementary Fig. S5D).

Therefore, transcriptomic correlates seem to correspond mostly to HS mutations, and the patterns of HS usage seem to be specific for multiple myeloma as compared with other solid and hematologic cancers.

Functional impact of biallelic events affecting tumor suppressor genes in multiple myeloma

Biallelic events carry an increasingly recognized prognostic effect in multiple myeloma. In particular, double-hit events occurring in tumor suppressor genes have been described to have a functional impact on cell fitness and survival and to represent the reservoir for disease relapse and drug resistance in more advanced stages (10–12, 39). Therefore, we sought to explore the transcriptomic consequences of biallelic events and how these are different from mono-allelic ones in key tumor suppressors: *FAM46C*, *DIS3*, *RB1*, *TGDS*, *TRAF3*, *CYLD*, and *TP53*.

To this end, we looked at genes with a cumulative effect, i.e., genes significantly deregulated in biallelic versus WT and/or biallelic versus mono-allelic statuses. Overall, among samples of patients with multiple myeloma the mono-allelic status was associated with little transcriptomic change as compared with WT, while biallelic events showed more profound changes (Supplementary Fig. S6; Supplementary Table S1 and Supplementary Data S3). Then, to better explain the putative functional impact of differential gene expression, we performed GO analysis on genes with a cumulative effect. As a common feature, we found a generalized upregulation of genes involved in cell-cycle regulation and cell proliferation. Interestingly, biallelic inactivations of *TP53*, *TGDS*, and *RB1* upregulated similar cyclins (*CCND2*, *CCNA2*, *CCNE2*) and spindle checkpoints genes (*E2F1* and *MCMs*). Furthermore, they shared also upregulation of aurora kinase-A (*AURKA*), cyclin-dependent kinases (*CDK1* and *CDK2*) and Polo-kinase-1 (*PLK1*), genes for which targeted treatments are being trialed (Supplementary Fig. S7). These results were confirmed by a GSEA. Indeed, we observed that cases with inactivation of *TP53*, *TGDS*, *RB1*, or *FAM46C* shared many cancer hallmarks gene sets, all related to cell-cycle regulation and MYC (Supplementary Fig. S8).

However, each gene aberration also showed a specific transcriptomic profile associated with biallelic inactivation. *CYLD* double-hit events showed as expected upregulation of downstream effectors of the NF-kB pathway such as *BIRC3*, *TRAF4*, *NFKB2*, *IKBKE*, *RELB*, and *TNFAIP3* (**Fig. 3A**, top; Supplementary Fig. S8). Moreover, we also detected an upregulation of genes involved in the interaction with microenvironment as *ICAM1*, *EDN1*, and *FGF2* related to angiogenesis enhancement (40), or *MIR146A* implicated in the communication with mesenchymal stromal cells. Interestingly, *CYLD* inactivation correlated with a significant overexpression of *BCL2*, with a cumulative effect for biallelic events (**Fig. 3A**, bottom). In the case of *TP53* double-

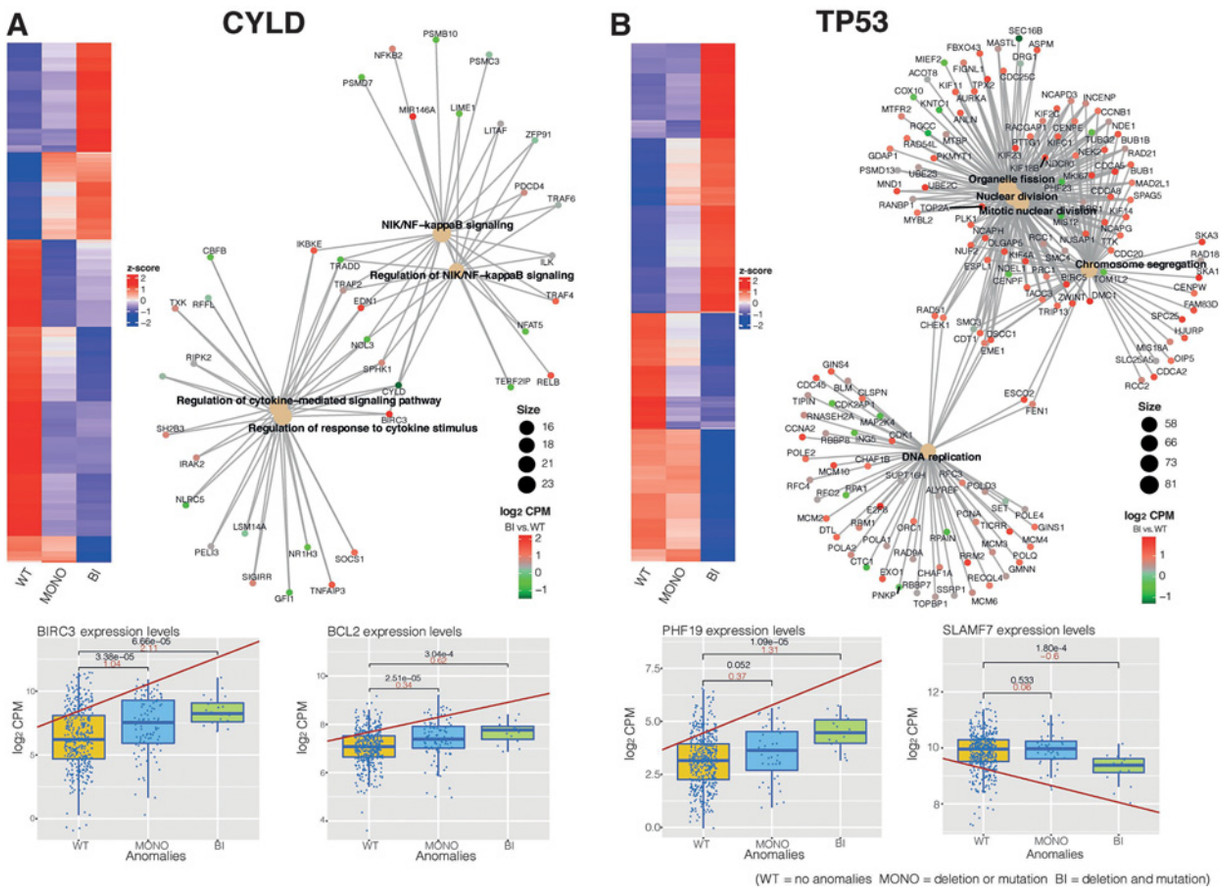

Figure 3.

Biallelic inactivation analysis. **A** and **B,** *CYLD* and *TP53* analysis. In the top left panel, the z-score value heatmaps of the cumulative effect genes, where columns represent the gene status and rows represent the genes. In the top right panel, the gene-network plot for cumulative effect genes, where big dots indicate the enriched pathways, small dots represent the deregulated genes, and the color-coding refers to the FC in biallelic versus WT contrast (log2CPM). In the lower panel, the box plots represent the cumulative gene expression trend in the three statuses, for each analysis: the dots specify the samples in each status, the red line symbolizes the trend of the gene expression, the red number denotes the incremental or decremental expression FC, the black number the *P* value.

hits, we noted an upregulation of cell-cycle genes as well as *PHF19*, a recently discovered poor prognostic marker in multiple myeloma (**Fig. 3B**; ref. 41). Therefore, we further explored this finding applying GSEA to dissect possible interactions between *TP53* inactivation and *PHF19* overexpression. Interestingly, the two abnormalities showed an overlap in upregulation of cell-cycle related and *MYC* controlled pathways (Supplementary Fig. S8), suggesting a convergence of mechanisms underlying poor prognosis in multiple myeloma. Furthermore, *TP53* double-hits were associated with downregulation of *SLAMF7*, an immunotherapeutic target in multiple myeloma (**Fig. 3B**, bottom). Interestingly, this was only observed in double-hit events and not when *TP53* was mutated or deleted only. *FAM46C* double-hit events were characterized by an upregulation of *CD38* and a concomitant low expression of *CD55* and *CD59*, recently associated with daratumumab resistance (Supplementary Fig. S7A) (42). Moreover, we found an upregulation of *CD44*, a gene involved in multiple myeloma cell homing and lenalidomide resistance (43). Then, we analyzed the impact of chr(13q) deletions and mutations of genes located within this region (Supplementary Fig. S7B–S7D). *TGDS* and *RB1* biallelic events deregulated mostly genes involved in cell-cycle and cell proliferation. Double-hit events of *TGDS* were predominantly associated with gene upregulation, while patients with *RB1* biallelic inactivations were characterized by differentially expressed genes in both directions compared with samples with normal/mono-allelic status of the gene. *DIS3* alterations correlated with increased expression of lncRNA regulatory genes (Supplementary Fig. S7B–S7D) as expected given its function (38). *TRAF3* inactivation was associated with NF-kB pathway activation and downregulation of signaling related to mRNA metabolic processes and protein catabolism (Supplementary Fig. S7E). Overall, these findings may help to explain the putative biological and prognostic impact of biallelic events in multiple myeloma.

Chromosome 1q gain/amplifications impacted transcriptome

Another recurrent CNA in multiple myeloma affects chr(1q21), where gains (3 copies) are thought to be early events and amplifications (4 or more copies) late events with a negative prognostic impact (11, 13). As for chromosomal deletions, also in this case we observed several genes characterized by a progressively increased change in expression in diploid versus gain versus amplifications of chr(1q21). While an intermediate differential expression was observed in the gain group compared with the disomic one, greater expression z-scores of these altered transcripts characterized the amplified cohort (**Fig. 4A**). As this was the single CNA with the largest number of transcriptomic correlates (**Fig. 1B**), we asked whether alteration of expression only impacted genes in the duplicated region or was genome-wide. Taking into account the number of differentially expressed genes in each chromosome corrected for the chromosomal length, we observed how small chromosomes (i.e., 21 or 22) contributed proportionally as much as chromosome 1 to transcriptomic changes between normal disomic configuration and 1q extra-copies. This suggests that chr(1q21)gain/amp may have profound implications on the transcriptome of the cell which are genome-wide (**Fig. 4B**). Subsequently, we applied a GO analysis on the genes with 1q CN-associated differential expression. Proliferation-related pathways, i.e., cell-cycle and spindle checkpoint genes were significantly upregulated (**Fig. 4C**). Chr(1q21)amp was associated with downregulation of *CCND1* and upregulation of *CCND2* along with other oncogenes (*AURKA*, *AURKB*, and *PLK1*) confirming the view that multiple myeloma is a disease of deregulated cyclins (Supplementary Fig. S9A and S9B; ref. 44). Given the known association between chr(1q21)gain/amp and t(4;14), we asked whether chr(1q21) amp effect on *CCND1* and *CCND2* could be mediated by t(4;14). Firstly, we noted that despite the presence of 1,102 shared differentially expressed genes between the two genetic abnormalities, chr(1q21)gain/amp was independently associated with 1,191 differentially expressed genes and t(4;14) with 3,841 (Supplementary Fig. S10A). Of note, while *CCND1* and *CCND2* were differentially expressed by both abnormalities, cases of chr(1q21)gain/amp without t(4;14) also showed *CCND2* upregulation (Supplementary Fig. S10B), confirming this is a convergent independent downstream effect of the two abnormalities and not a confounding effect of their association. Other than this, a GO analysis of differentially expressed genes specific to each genetic abnormality did not show shared deregulated pathways (Supplementary Fig. S10C and S10D). Finally, several genes with a possible therapeutic impact were differentially expressed. In particular, *PDL1* was downregulated, while the immunotherapy targets *SLAMF7* and *GPRC5D* were significantly overexpressed (**Fig. 4D**; Supplementary Fig. S9C). Of note, the chromosome 1q amplification was also associated with a significant upregulation of *MCL1* (**Fig. 4E**), whose overexpression is associated with a lower response to BCL2 inhibition. Altogether, these data confirmed the high impact that chromosome 1q alterations have on the transcriptome and of great importance are the highly significant expression changes on genes with possible therapeutical implication for new generation immunotherapies (*SLAMF7* and *GPRC5D)* or targeted treatments (*MCL1*).

Structural chromosomal alterations as possible predictors of response to BCL2 inhibitors

Venetoclax is becoming a commonly used therapeutic approach in hematological malignancies and shows great promise in the multiple myeloma field as well (22, 45, 46). Nevertheless, in multiple myeloma venetoclax use seems to only be beneficial for certain subgroups of patients and is detrimental for others, making it crucial to identify reliable biomarkers (47). Studies have highlighted the *BCL2*/*MCL1* and *BCL2*/*BCL2L1* expression ratios as predictors of response (48). However, in routine clinical practice these analyses are not performed and venetoclax use is confined to the t(11;14) setting, as these cases express high levels of BCL2 (22, 48). Since *BCL2* overexpression seems not to be confined to t(11;14) cases, we mined our data to look for additional genomic predictors of response to venetoclax studying the expression levels of *BCL2*, *MCL1*, and *BCL2L1*. Interestingly, as described in mouse models (49), *CYLD*-deleted cases showed the most significant upregulation of *BCL2*, while t(11;14) cases did not cross our FDR threshold (Supplementary Table S2) for *BCL2* expression unless associated with del(*CYLD*). In t(11;14), the most notable feature was a downregulation of *BCL2L1*. Conversely, chr(1q21)gain/amps alone or in association with chr(13) deletions were characterized by an overexpression of *MCL1* (Supplementary Table S2 and **Fig. 5**), likely explaining resistance to venetoclax of chr(1q) cases, who, by contrast, are highly sensitive to MCL1 targeting (50). Indeed, among *BCL2* overexpressing cases, there was an enrichment of t(11;14) and del(*CYLD*) (Supplementary Fig. S11A). *MCL1* expression was characterized by an enrichment of chr(1q)gain/amps among high-expressors (Supplementary Fig. S11B). In the case of *BCL2L1*, it was clearly seen how most cases with low expression were indeed characterized by t(11;14) (Supplementary Fig. S11C). Concerning expression ratios, chr(1q)gain/amps were associated with a significant reduction of the *BCL2*/*MCL1* ratio. On the other hand, the *BCL2*/*BCL2L1* ratio was very high in the t(11;14) setting, explaining the positive effect of venetoclax in this subgroup (Supplementary Table S3).

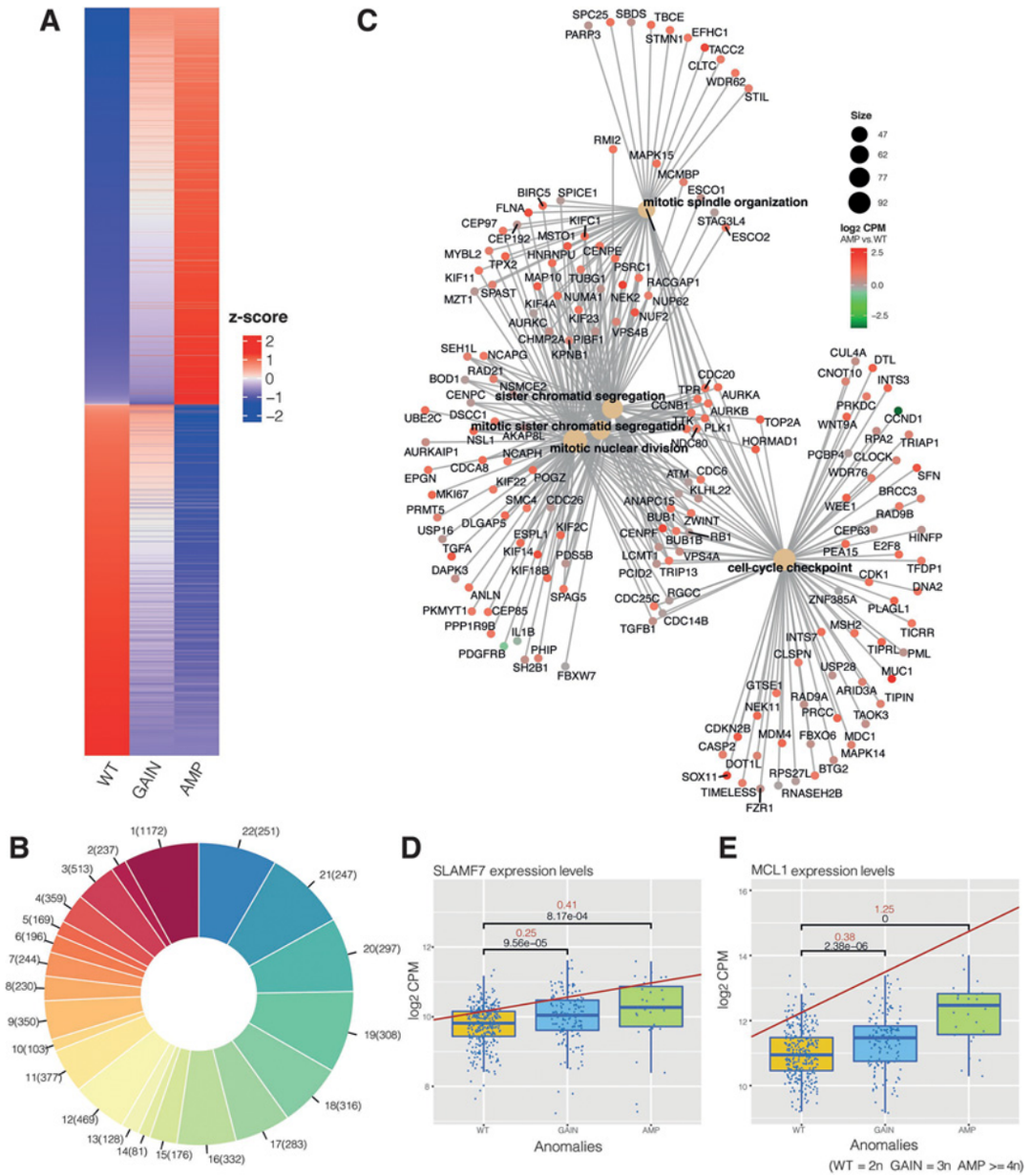

Figure 4.

Chromosome 1q gain/amplification analysis. **A,** The heatmap represents the z-score values for the cumulative effect genes. **B,** The pie chart represents the chromosomal distribution of the cumulative effect genes, corrected for chromosomal length. **C,** Gene-network plot for cumulative effect genes, related to the amplification versus WT contrast (log2CPM). **D,** Box plot for the *SLAMF7* expression trend in the three statuses. **E,** Box plot for *MCL1* expression trend.

In conclusion, we observed genetic lesions that are associated with a peculiar modulation of expression of genes related to the BCL2 pathway which could translate into biomarkers for venetoclax treatment.

In silico drug sensitivity screening shows that t(11;14) is not the only predictor for venetoclax response

The above results highlighted some genotype–phenotype correlations that may predict response to BCL2 pathway inhibitors. To validate these findings *in silico*, we interrogated public datasets generated within the DepMap international collaboration, reporting on genetic dependencies and small molecule sensitivities of about 2,000 cancer cell lines (33, 34). To select the most appropriate cell lines for our analysis, we used the *Celligner* algorithm (35). This allowed the comparison of transcriptomic data from DepMap cell lines and multiple myeloma samples from CoMMpass, and therefore the selection of the cell lines most similar to our primary sample data. Multiple myeloma cell lines are characterized by specific IGH rearrangements, and *Celligner* correctly clustered them with multiple myeloma samples harboring the same translocation (**Fig. 6A**). Interestingly, even if

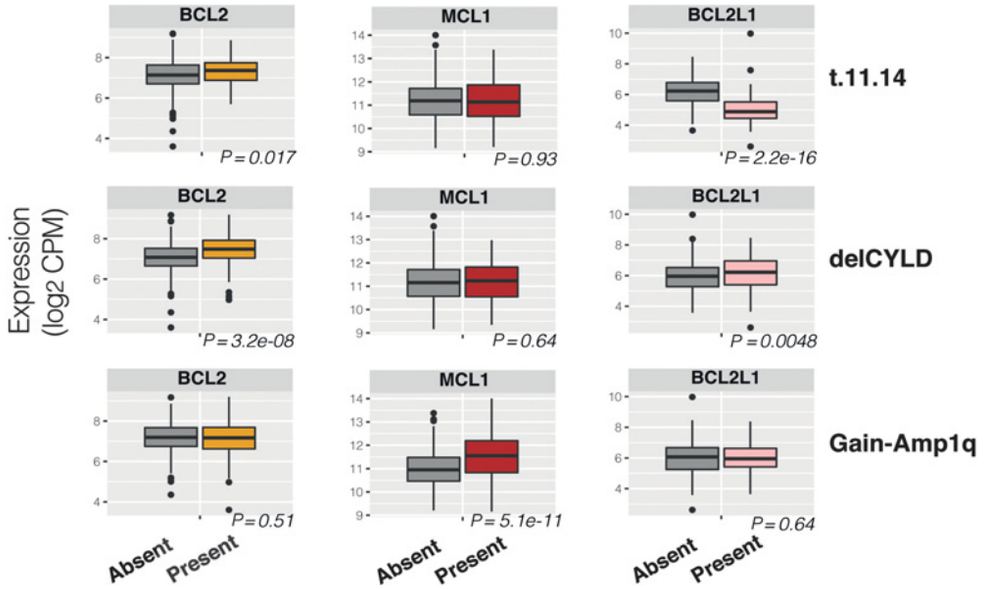

Figure 5.
BCL2 family gene expression analysis. Box plots representing the specific BCL2 family gene expression in t(11;14), del(*CYLD*), and chr(1q21)gain/amps samples.

HDMM cell lines are hardly reported, many cell lines were anchored with samples of patients with HDMM, which may have translational relevance. Analysis of genomic and expression data showed that this was not due to *MYC* translocation or overexpression. In the sample space defined by *Celligner* we selected cell lines harboring the three chromosomal abnormalities that we identified above as possible predictors of venetoclax response (features of cell lines are summarized in Supplementary Table S4). The cell line GRANTA519 and multiple myeloma cell lines SKMM2 and KMS12BM harbor a t(11;14) translocation, and a *CYLD* deletion in the latters. As expected, these three cell lines resulted highly sensitive to venetoclax treatment (**Fig. 6B–D**). Then, we interrogated the dataset for the U266 and MOLP8 multiple myeloma cell lines, both carrying a t(11;14). Notably, these two models showed refractoriness to BCL2 inhibition (**Fig. 6E** and **F**), most likely since they are both characterized by high expression of *MCL1* due to chr(1q)gain/amp, and *BCL2L1* gain in the case of U266. The only cell line in DepMap with an isolated del(*CYLD*) was the RI1, and it was sensitive to venetoclax (**Fig. 6G**). To gain further evidence that del(*CYLD*) could predict venetoclax response, we analyzed public data on venetoclax sensitivity reported in recent papers (50–52). By integrating these drug sensitivity data and genomic information retrieved from literature and publicly available repositories, we were able to report the characteristics of 53 additional multiple myeloma cell lines (Supplementary Table S5). Five of these harbored a del(*CYLD*), but this was isolated only in PCM6 and in the remaining 4 lines was associated with chr(1q21)gain/amps. Adding independent evidence to our hypothesis, the PCM6 cell line resulted highly sensitive to venetoclax (51), while the others were resistant likely due to *MCL1* overexpression. In fact, the MCL1 inhibitor S63845 was tested in the AMO1 cell line harboring a chr(1q) amplification and resulted in decreased viability (50). However, the complex genotype of cell lines and the many genetic and epigenetic variables affecting expression represent major challenges to the discovery and wider applicability of candidate biomarkers of venetoclax sensitivity, and validation by functional studies will clearly be required. Extensive mining of geno-transcriptomic data and cancer dependencies may increase the spectrum of candidate biomarkers of venetoclax sensitivity in multiple myeloma.

Discussion

In this study, we systematically dissected the impact of well known and more recently described genome-wide DNA abnormalities on the expression profile of 514 multiple myeloma cases to identify putative functional correlates and surrogates of gene expression that may have translational implications. As expected, and confirming the validity of our approach, we found that hyperdiploidy and recurrent IGH translocations were associated with the most substantial differential gene expression patterns between patients. The assessment of the transcriptomic profiles associated with any recurrent CNA and gene mutation, representing a hallmark of our analysis, highlighted novel correlates, by means of which we could also identify specific lesions worthy of investigation in clinical-grade diagnostics for their potential implications on patient management. Overall, gene mutations carried a lower transcriptomic impact. This may be explained by the fact that most show instances of convergent evolution (e.g., mutually exclusive mutations of *KRAS* and *NRAS*), do not segregate with specific genomic lesions, and are often subclonal. Therefore, their impact may be diffuse and redundant, and furthermore diluted when analyzing bulk sequencing data. Interestingly though, functional relevance seems to be only attributable to hotspot mutations for the two most common mutated genes *KRAS* and *NRAS*, and their hotspot usage is quite different between multiple myeloma and other solid cancers. This finding may have functional implications that need to be further studied. A questionable driver event is represented by *IGLL5* mutations, as they are mostly seen as off-target AID-induced mutations (53). The fact that in our analysis *IGLL5* mutations are not associated with the differential expression of any transcript strongly supports this view. However, they could be a marker of IGL translocations and poor prognosis (2).

The single CNA associated with the largest number of transcriptomic correlates was chr(1q21), where gains and, to a more extent, amplifications predicted downregulation of *PDL1* and upregulation of

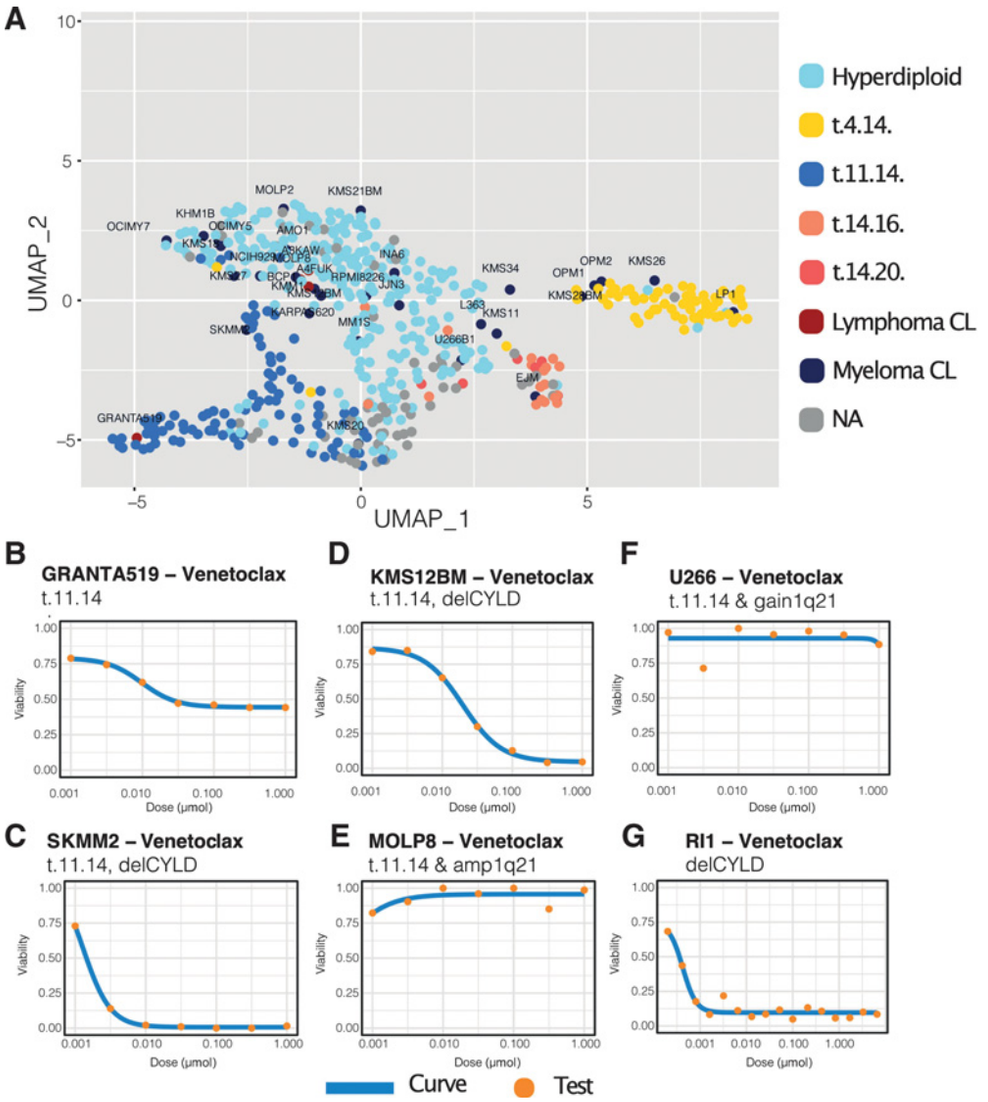

Figure 6.

In silico drug sensitivity screen. **A,** UMAP 2D projection of *Celligner*-aligned sample and cell line expression data: dots represent the samples [HD in light blue, t(4;14) in yellow, t(11;14) in blue, t(14;16) in salmon, and t(14;20) in pink] and the lymphoma (dark blue) and myeloma (red) cell lines, samples missing karyotype in gray. **B–G,** Dose–response curves for cell lines of interest: orange dots represent tests and blue curves represent the fitted trends. *drc*, *dr4pl* R packages have been used to generate drug-sensitivity plots.

SLAMF7, *GPRC5D*, and *MCL1*, with clear implications for treatment with immunotherapies and BCL2 inhibitors. Overall, chr(1q21)gain/amp corresponded to a transcriptional modulation that was genome-wide and not limited to that genomic region, and was associated with the upregulation of a proliferative program driven by CCND2 and other oncogenes. Indeed, a similar pattern has been reported by RNA-seq of proteasome inhibitors (PI) and immunomodulatory agents double-refractory cases (7), making chr(1q)gain/amp one of the worst prognostic markers even in the era of novel treatments (54). Of note, transcriptomic changes associated with chr(1q21) were much more profound in case of amplifications than gains. This was an overall very notable trend also for tumor suppressor lesions, where most of the transcriptomic changes were found associated with biallelic events (i.e., mutation of one allele and deletion of the other). Some of these had therapeutic correlates, such as NF-kB pathway upregulation in *TRAF3* and *CYLD* inactivation, predicting good response to PI treatment (55, 56). Others had prognostic value, such as *PHF19* upregulation that was seen upon *TP53* biallelic loss (41).

Most importantly, we identified potential genomic correlates of response to BCL2 pathway inhibitors. While response to venetoclax is best associated with a high *BCL2*/*MCL1* or *BCL2*/*BCL2L1* ratio, this is rarely assessed in the clinic, and the easier to identify t(11;14) translocation is the typical biomarker used to select patients that may respond to venetoclax. Our data show how t(11;14) patients display high *BCL2* levels and lack chr(1q21)gain/amp events thus showing low *MCL1* levels. However, their sensitivity to venetoclax is best explained by their consistently low *BCL2L1* levels. In our *in silico* analysis, t(11;14) was found associated with resistance to venetoclax therapy in 2 cell lines,

where it cooccurred with amplification of 1q and high expression of *MCL1*. In this setting, Slomp and colleagues have shown how 1q amplifications could identify a high-risk patient subset suitable for therapy with specific MCL1 inhibitors. Interestingly, the authors have also shown how the combinatorial therapy with BCL2 and MCL1 antagonists could overcome venetoclax resistance in human myeloma cell lines as well as the newly diagnosed patients (50). Of note, the double inhibition leads to the formation of proapoptotic BAX-BAK heterocomplexes promoting apoptosis activation (52), and this could be the mechanism restoring apoptosis in these cells. Our systematic analysis also allowed to identify other DNA lesions that may predict venetoclax response, and among these are *CYLD* deletions. These are not significantly associated with t(11;14) (10, 14), and are associated with the highest *BCL2* levels of the CoMMpass cohort. Consistently, our functional *in silico* validation confirmed that del(*CYLD*) cell lines respond to venetoclax and that this could represent a candidate biomarker to identify patients who could respond to BCL2 inhibition. Nevertheless, within multiple myeloma cell lines, *CYLD* deletions were more variably associated with venetoclax sensitivity, owing to complex karyotypes with additional chromosomal abnormalities involving *BCL2* losses and chr(1q21)gain/amp associated with high *MCL1* expression. Therefore, while our data from primary samples recapitulate *in vivo* mouse models where *CYLD* knockdown resulted in *BCL2* upregulation (49), the translation of this evidence into a suitable biomarker of venetoclax sensitivity in the context of plasma cell neoplasms is hampered by the scanty cell line models with a clean genetic background, and likely by nongenetic mechanisms of resistance (57), and will require additional studies. In search for additional predictors of venetoclax sensitivity, Gupta and colleagues recently highlighted a new gene/antigen signature that is independent of t(11;14) (51), and whose clinical utility will need testing.

Altogether, our study highlights the impact of detailed molecular profiling partnered with clinical annotations and how, when combined with large datasets of patients, this can be leveraged to study outcomes of targeted drugs in well defined biological subgroups of patients with multiple myeloma.

Authors' Disclosures

S. Oliva reports personal fees from Celgene/BMS, Janssen, and Amgen outside the submitted work. M. D'Agostino reports personal fees from Sanofi and GSK outside the submitted work. O. Landgren reports grants and personal fees from Amgen, Janssen, Karyopharm, and Binding Site; grants from Celgene, Takeda, MMRF, Perelman Family Foundation, and NCI; personal fees from Adaptive Biotech, Bristol-Myers Squibb, Cellectis, Oncopeptides, and Pfizer; and other support from Janssen, Theadex, and Merck outside the submitted work. F. Iorio reports grants from Open Targets and other support from Joint CRUK-AstraZeneca Functional Genomics Center outside the submitted work. N. Bolli reports grants from European Research Council during the conduct of the study as well as personal fees from Celgene-BMS, Janssen, Amgen, and Takeda outside the submitted work. No disclosures were reported by the other authors.

Authors' Contributions

B. Zicchedda: Data curation, software, formal analysis, validation, visualization, methodology, writing–original draft. **M.C. Da Vià:** Data curation, formal analysis, validation, visualization, methodology, writing–original draft, writing–review and editing. **M. Lionetti:** Data curation, formal analysis, validation, visualization, methodology, writing–review and editing. **A. Maeda:** Investigation, methodology. **S. Morlupi:** Investigation, methodology. **M. Dugo:** Software, formal analysis, methodology. **K. Todoerti:** Software, formal analysis, methodology. **S. Oliva:** Data curation, methodology. **M. D'Agostino:** Data curation, methodology. **P. Corradini:** Data curation. **O. Landgren:** Data curation. **F. Iorio:** Software, supervision, visualization. **L. Pettine:** Data curation. **A. Pompa:** Data curation. **M. Manzoni:** Software, formal analysis, investigation, methodology. **L. Baldini:** Supervision. **A. Neri:** Supervision, funding acquisition. **F. Maura:** Conceptualization, supervision, writing–review and editing. **N. Bolli:** Conceptualization, resources, supervision, funding acquisition, project administration, writing–review and editing.

Acknowledgments

This work was supported by the European Research Council under the European Union's Horizon 2020 research and innovation program (817997, to N. Bolli), Associazione Italiana Ricerca sul Cancro (IG16722, IG10136 and IG24365 to A. Neri, IG20541), the Multiple Myeloma Research Foundation (MMRF; to F. Maura), the Perelman Family Foundation (to O. Landgren), the Riney Family Multiple Myeloma Research Program Fund (to O. Landgren), a Memorial Sloan Kettering Cancer Center NCI Core Grant (P30 CA 008748, to O. Landgren), and a Sylvester Comprehensive Cancer Center NCI Core Grant (P30 CA 240139, to O. Landgren). F. Maura is supported by the American Society of Hematology.

The costs of publication of this article were defrayed in part by the payment of page charges. This article must therefore be hereby marked *advertisement* in accordance with 18 U.S.C. Section 1734 solely to indicate this fact.

Received November 7, 2020; revised February 22, 2021; accepted September 9, 2021; published first September 15, 2021.

References

1. Morgan GJ, Walker BA, Davies FE. The genetic architecture of multiple myeloma. Nat Rev Cancer 2012;12:335–48.
2. D'Agostino M, Zaccaria GM, Zicchedda B, Rustad EH, Genuardi E, Capra A, et al. Early relapse risk in patients with newly diagnosed multiple myeloma characterized by next-generation sequencing. Clin Cancer Res 2020;26:4832–41.
3. Keats JJ, Chesi M, Egan JB, Garbitt VM, Palmer SE, Braggio E, et al. Clonal competition with alternating dominance in multiple myeloma. Blood 2012;120:1067–76.
4. Samur MK, Samur AA, Fulciniti M, Szalat R, Han T, Shammas M, et al. Genome-wide somatic alterations in multiple myeloma reveal a Superior Outcome Group. J Clin Oncol 2020;38:3107–18.
5. Da Via MC, Zicchedda B, Maeda A, Bagnoli F, Perrone G, Bolli N. A journey through myeloma evolution: From the normal plasma cell to disease complexity. Hemasphere 2020;4:e502.
6. Bolli N, Maura F, Minvielle S, Gloznik D, Szalat R, Fullam A, et al. Genomic patterns of progression in smoldering multiple myeloma. Nat Commun 2018;9:3363.
7. Zicchedda B, Biancon G, Bagnoli F, De Philippis C, Maura F, Rustad EH, et al. Integrative analysis of the genomic and transcriptomic landscape of double-refractory multiple myeloma. Blood Adv 2020;4:830–44.
8. Oben B, Froyen G, Maclachlan KH, Leongamornlert D, Abascal F, Zheng-Lin B, et al. Whole-genome sequencing reveals progressive versus stable myeloma precursor conditions as two distinct entities. Nat Commun 2021;12:1861.
9. Neuse CJ, Lomas OC, Schliemann C, Shen YJ, Manier S, Bustoros M, et al. Genome instability in multiple myeloma. Leukemia 2020;34:2887–97.
10. Bolli N, Biancon G, Moarii M, Gimondi S, Li Y, de Philippis C, et al. Analysis of the genomic landscape of multiple myeloma highlights novel prognostic markers and disease subgroups. Leukemia 2018;32:2604–16.
11. Walker BA, Mavrommatis K, Wardell CP, Ashby TC, Bauer M, Davies F, et al. A high-risk, Double-Hit, group of newly diagnosed myeloma identified by genomic analysis. Leukemia 2019;33:159–70.
12. Weinhold N, Ashby C, Rasche L, Chavan SS, Stein C, Stephens OW, et al. Clonal selection and double-hit events involving tumor suppressor genes underlie relapse in myeloma. Blood 2016;128:1735–44.
13. Maura F, Bolli N, Angelopoulos N, Dawson KJ, Leongamornlert D, Martincorena I, et al. Genomic landscape and chronological reconstruction of driver events in multiple myeloma. Nat Commun 2019;10:3835.
14. Walker BA, Mavrommatis K, Wardell CP, Ashby TC, Bauer M, Davies FE, et al. Identification of novel mutational drivers reveals oncogene dependencies in multiple myeloma. Blood 2018;132:587–97.

15. Hideshima T, Bergsagel PL, Kuehl WM, Anderson KC. Advances in biology of multiple myeloma: clinical applications. Blood 2004;104:607–18.
16. Mattioli M, Agnelli L, Fabris S, Baldini L, Morabito F, Bicciato S, et al. Gene expression profiling of plasma cell dyscrasias reveals molecular patterns associated with distinct IGH translocations in multiple myeloma. Oncogene 2005;24: 2461–73.
17. Zhan F, Huang Y, Colla S, Stewart JP, Hanamura I, Gupta S, et al. The molecular classification of multiple myeloma. Blood 2006;108:2020–8.
18. Cleynen A, Szalat R, Samur MK, du Pont SR, Buisson L, Boyle E, et al. Expressed fusion gene landscape and its impact in multiple myeloma. Nat Commun 2017; 8:1893.
19. Foltz SM, Gao Q, Yoon CJ, Sun H, Yao L, Li Y, et al. Evolution and structure of clinically relevant gene fusions in multiple myeloma. Nat Commun 2020; 11:2666.
20. Lagana A, Perumal D, Melnekoff D, Readhead B, Kidd BA, Leshchenko V, et al. Integrative network analysis identifies novel drivers of pathogenesis and progression in newly diagnosed multiple myeloma. Leukemia 2018;32:120–30.
21. Rashid NU, Sperling AS, Bolli N, Wedge DC, Van Loo P, Tai YT, et al. Differential and limited expression of mutant alleles in multiple myeloma. Blood 2014;124:3110–7.
22. Kumar S, Kaufman JL, Gasparetto C, Mikhael J, Vij R, Pegourie B, et al. Efficacy of venetoclax as targeted therapy for relapsed/refractory t(11;14) multiple myeloma. Blood 2017;130:2401–9.
23. Bolli N, Genuardi E, Zicchedu B, Martello M, Oliva S, Terragna C. Next-generation sequencing for clinical management of multiple myeloma: Ready for prime time? Front Oncol 2020;10:189.
24. Bolli N, Li Y, Sathiaseelan V, Raine K, Jones D, Ganly P, et al. A DNA target-enrichment approach to detect mutations, copy number changes and immunoglobulin translocations in multiple myeloma. Blood Cancer J 2016;6:e467.
25. Yellapantula V, Hultcrantz M, Rustad EH, Wasserman E, Londono D, Cimera R, et al. Comprehensive detection of recurring genomic abnormalities: a targeted sequencing approach for multiple myeloma. Blood Cancer J 2019;9:101.
26. Ritchie ME, Phipson B, Wu D, Hu Y, Law CW, Shi W, et al. limma powers differential expression analyses for RNA-sequencing and microarray studies. Nucleic Acids Res 2015;43:e47.
27. Law CW, Chen Y, Shi W, Smyth GK. voom: Precision weights unlock linear model analysis tools for RNA-seq read counts. Genome Biol 2014;15:R29.
28. Robinson MD, Oshlack A. A scaling normalization method for differential expression analysis of RNA-seq data. Genome Biol 2010;11:R25.
29. Gerstung M, Pellagatti A, Malcovati L, Giagounidis A, Porta MG, Jadersten M, et al. Combining gene mutation with gene expression data improves outcome prediction in myelodysplastic syndromes. Nat Commun 2015;6:5901.
30. Chang MT, Asthana S, Gao SP, Lee BH, Chapman JS, Kandoth C, et al. Identifying recurrent mutations in cancer reveals widespread lineage diversity and mutational specificity. Nat Biotechnol 2016;34:155–63.
31. Yu G, Wang LG, Han Y, He QY. clusterProfiler: an R package for comparing biological themes among gene clusters. OMICS 2012;16:284–7.
32. Subramanian A, Tamayo P, Mootha VK, Mukherjee S, Ebert BL, Gillette MA, et al. Gene set enrichment analysis: a knowledge-based approach for interpreting genome-wide expression profiles. Proc Natl Acad Sci U S A 2005;102:15545–50.
33. Iorio F, Knijnenburg TA, Vis DJ, Bignell GR, Menden MP, Schubert M, et al. A Landscape of Pharmacogenomic Interactions in Cancer. Cell 2016;166:740–54.
34. Tsherniak A, Vazquez F, Montgomery PG, Weir BA, Kryukov G, Cowley GS, et al. Defining a cancer dependency map. Cell 2017;170:564–76.
35. Warren A, Chen Y, Jones A, Shibue T, Hahn WC, Boehm JS, et al. Global computational alignment of tumor and cell line transcriptional profiles. Nat Commun 2021;12:22.
36. Agnelli L, Bicciato S, Mattioli M, Fabris S, Intini D, Verdelli D, et al. Molecular classification of multiple myeloma: a distinct transcriptional profile characterizes patients expressing CCND1 and negative for 14q32 translocations. J Clin Oncol 2005;23:7296–306.
37. Zhou Y, Zhang Q, Stephens O, Heuck CJ, Tian E, Sawyer JR, et al. Prediction of cytogenetic abnormalities with gene expression profiles. Blood 2012;119: e148–50.
38. Lionetti M, Barbieri M, Todoerti K, Agnelli L, Fabris S, Tonon G, et al. A compendium of DIS3 mutations and associated transcriptional signatures in plasma cell dyscrasias. Oncotarget 2015;6:26129–41.
39. Munawar U, Rasche L, Muller N, Vogt C, Da-Via M, Haertle L, et al. Hierarchy of mono- and biallelic TP53 alterations in multiple myeloma cell fitness. Blood 2019;134:836–40.
40. Solimando AG, Da Via MC, Leone P, Borrelli P, Croci GA, Tabares P, et al. Halting the vicious cycle within the multiple myeloma ecosystem: blocking JAM-A on bone marrow endothelial cells restores angiogenic homeostasis and suppresses tumor progression. Haematologica 2021;106:1943–56.
41. Ren Z, Ahn JH, Liu H, Tsai YH, Bhanu NV, Koss B, et al. PHF19 promotes multiple myeloma tumorigenicity through PRC2 activation and broad H3K27me3 domain formation. Blood 2019;134:1176–89.
42. Nijhof IS, Casneuf T, van Velzen J, van Kessel B, Axel AE, Syed K, et al. CD38 expression and complement inhibitors affect response and resistance to daratumumab therapy in myeloma. Blood 2016;128:959–70.
43. Bjorklund CC, Baladandayuthapani V, Lin HY, Jones RJ, Kuiatse I, Wang H, et al. Evidence of a role for CD44 and cell adhesion in mediating resistance to lenalidomide in multiple myeloma: therapeutic implications. Leukemia 2014; 28:373–83.
44. Bergsagel PL, Kuehl WM, Zhan F, Sawyer J, Barlogie B, Shaughnessy J Jr.Cyclin D dysregulation: an early and unifying pathogenic event in multiple myeloma. Blood 2005;106:296–303.
45. DiNardo CD, Jonas BA, Pullarkat V, Thirman MJ, Garcia JS, Wei AH, et al. Azacitidine and venetoclax in previously untreated acute myeloid leukemia. N Engl J Med 2020;383:617–29.
46. Roberts AW, Davids MS, Pagel JM, Kahl BS, Puvvada SD, Gerecitano JF, et al. Targeting BCL2 with venetoclax in relapsed chronic lymphocytic leukemia. N Engl J Med 2016;374:311–22.
47. Kumar S, Harrison SJ, Cavo C, De La Rubia J, Popat R, Gasparetto C, et al. Updated results from BELLINI, a phase III study of venetoclax or placebo in combination with bortezomib and dexamethasone in relapsed/refractory multiple myeloma. J Clin Oncol 38;15s, 2020.
48. Touzeau C, Maciag P, Amiot M, Moreau P. Targeting Bcl-2 for the treatment of multiple myeloma. Leukemia 2018;32:1899–907.
49. Hovelmeyer N, Wunderlich FT, Massoumi R, Jakobsen CG, Song J, Worns MA, et al. Regulation of B cell homeostasis and activation by the tumor suppressor gene CYLD. J Exp Med 2007;204:2615–27.
50. Slomp A, Moesbergen LM, Gong JN, Cuenca M, von dem Borne PA, Sonneveld P, et al. Multiple myeloma with 1q21 amplification is highly sensitive to MCL-1 targeting. Blood Adv 2019;3:4202–14.
51. Gupta VA, Barwick BG, Matulis SM, Shirasaki R, Jaye DL, Keats JJ, et al. Venetoclax sensitivity in multiple myeloma is associated with B-cell gene expression. Blood 2021;137:3604–15.
52. Seiller C, Maiga S, Touzeau C, Bellanger C, Kervoelen C, Descamps G, et al. Dual targeting of BCL2 and MCL1 rescues myeloma cells resistant to BCL2 and MCL1 inhibitors associated with the formation of BAX/BAK hetero-complexes. Cell Death Dis 2020;11:316.
53. Maura F, Rustad EH, Yellapantula V, Luksza M, Hoyos D, Maclachlan KH, et al. Role of AID in the temporal pattern of acquisition of driver mutations in multiple myeloma. Leukemia 2020;34:1476–80.
54. Abdallah N, Greipp P, Kapoor P, Gertz MA, Dispenzieri A, Baughn LB, et al. Clinical characteristics and treatment outcomes of newly diagnosed multiple myeloma with chromosome 1q abnormalities. Blood Adv 2020;4:3509–19.
55. Annunziata CM, Davis RE, Demchenko Y, Bellamy W, Gabrea A, Zhan F, et al. Frequent engagement of the classical and alternative NF-kappaB pathways by diverse genetic abnormalities in multiple myeloma. Cancer Cell 2007;12:115–30.
56. Keats JJ, Fonseca R, Chesi M, Schop R, Baker A, Chng WJ, et al. Promiscuous mutations activate the noncanonical NF-kappaB pathway in multiple myeloma. Cancer Cell 2007;12:131–44.
57. Neri P, Maity R, Alberge J, Sinha S, Donovan J, Kong M, et al. Mutations and copy number gains of the BCL2 family members mediate resistance to venetoclax in multiple myeloma (MM) patients. In: Proceedings of the American Society of Hematology Annual meeting; 2019; San Diego, CA. Blood; 2019.